Current Science
CS 4 (6), 894– 902 (2024)
Received 24 Sept 2024 | **Revised** 25 Oct 2024 | **Accepted** 26 Nov. 2024 | **Online Available** 10 Dec 2024
https://doi.org/10.52845/CS/2024-4-6-12

Current Science

Current Science

OPEN ACCESS

ISSN(O)2795-8639

ORIGINAL ARTICLE

Research on Slight Decarburization Grinding Hardening Based on the Gas-Protecting Coupling Method

Xiao-Liang Shi[1,*] ·Xiao Liu[2]

[1]School of Physics, Liaoning University, Shenyang, 110819, China

[2]Library, Northeastern University, Shenyang, 110819, China

*Corresponding Author: Xiao-Liang Shi, Xiao Liu

Abstract
This study advances the field of abrasive machining with a novel gas-protecting coupling method designed to control decarburization during the grinding hardening process. Traditional grinding hardening, while effective for imparting surface hardness, can cause decarburization, leading to a loss of material properties such as toughness and fatigue strength. To mitigate this, a method is proposed that employs a nitrogen gas shield to protect the workpiece surface from reactive atmospheric gases. An experimental platform is developed allowing for the application of nitrogen gas during grinding. The results from 45 steel workpiece demonstrated that the gas-protected grinding hardening process preserves carbon content at the surface. Computational fluid dynamics simulations were conducted to analyze the airflow-field interaction, providing insights that led to the optimization of the gas injection strategy. Additionally, a deep neural network model was trained to predict carbon content variations, supporting the precision control of the decarburization process. Collectively, these findings offer a significant contribution towards greener and more efficient manufacturing processes for carbon steel components.
Keywords Grinding Hardening, Decarburization, Gas Protection, Surface Properties, Airflow-field, Neural Network.

Introduction

Grinding hardening technology, a green composite processing method that seamlessly integrates grinding and surface quenching, is originally conceived by the visionary duo of Brinksmeier and Brockhoff from Germany in the 1990[1]. This innovative approach exploits the abundant grinding heat and intense mechanical forces generated within the contact zone during the grinding process, particularly under rigorous conditions of profound cutting depths and the absence of coolant[2-4]. By harnessing these energies directly, the technology achieves surface quenching of steel components, resulting in a pronounced hardening and strengthening effect on the machined surface. Notably, grinding hardening technology efficiently capitalizes on the otherwise wasted grinding heat, enhancing the surface strength and hardness of the finished workpiece[5-8]. This integration of grinding and surface heat treatment into a single process not only elevates energy utilization efficiency but also ensures high-precision surface machining. Furthermore, it imparts a hardening effect to the machined surface, thereby enhancing the overall performance and durability of the component. Given its eco-friendly, energy-efficient, and high-performance characteristics, grinding hardening technology has garnered widespread attention and research interest from scholars both domestically and internationally since its inception. Its potential to revolutionize metalworking practices and contribute to sustainable manufacturing makes it a field of immense research value and practical significance[9-12].

However, during the process of grinding hardening, due to the large amount of grinding heat generated in the grinding contact area, the carbon element activity becomes stronger, and the components such as O_2, CO_2, H_2O and H_2 in the air easily react with the solid solution carbon on the steel surface, resulting in gas overflowing out of the steel, which reduces the carbon concentration on the steel surface and causes decarburization[13]. Surface decarburization behavior has an important influence on workpiece[14]. After decarburization, the surface toughness of the workpiece is reduced, the surface becomes brittle, the fatigue strength is greatly reduced, and the service life of the workpiece is greatly shortened; The surface hardness decreases and the wear resistance is greatly weakened. Under the condition of grinding hardening, the original hardening effect is affected. These adverse effects restrict the long-term service and service performance of ground hardened workpiece. Other fields of metal hot working and heat treatment try their best to avoid decarburization, especially in the treatment of important workpiece[15, 16]. The surface decarburization behavior has not been paid enough attention in the past research on grinding hardening, and there are few reports on the surface decarburization phenomenon of grinding hardening. On the premise of reasonable manufacturability and economy, if targeted measures can be taken to control the decarburization behavior of the surface of workpiece during grinding hardening, the performance of grinding hardening layer will be greatly optimized, and the efficiency of grinding and workpiece will be greatly improved.

Based on the above analysis, aiming at the decarburization phenomenon of workpiece surface in the process of grinding and hardening, combined with the common controlling principle of decarburization in industry and the characteristics of grinding, this paper innovatively puts forward a machining method based on gas shielding to realize the decarburization control of grinding hardening surface which is the slight decarburization grinding hardening based on the gas-protecting coupling method. On the premise of satisfying manufacturability, environmental protection and economy, a follow-up protective gas injection module is designed and developed, which takes inert gas nitrogen as protective gas. In the grinding hardening process, the protective gas bath formed by the injected gas is used to avoid the gas factors inducing decarburization effect, and protect the surface of the workpiece to complete the compound grinding hardening process, forming a slightly decarburized or non-decarburized hardening layer.

The analysis underscores the criticality of investigating micro-decarburization hardening grinding with gas composite protection in the realm of abrasive machining. This approach offers a promising avenue to comprehensively enhance the surface mechanical properties of machined components and elevate the overall machining effectiveness. By delving into the intricate mechanisms of this process, researchers can unlock significant breakthroughs that transcend traditional methods. Drawing upon the theories of fluid dynamics, metallurgy, and grinding mechanics, the establishment of a systematic model for decarburization control methods, coupled with a predictive mechanism for comprehensive decarburization capacity, represents a pivotal step forward. This integrated framework not only facilitates precision machining but also optimizes the service life of critical carbon steel workpiece by minimizing decarburization. The result is a refined surface quality that exceeds conventional grinding standards, offering a fresh perspective and innovative solution for enhancing the durability and performance of precision-engineered components. In essence, this research endeavor presents a paradigm shift in the field of surface grinding, paving the way for new possibilities in surface quality enhancement.

2 Experiment study of slight decarburization grinding hardening

2.1 Establishment of experimental platform

An experimental platform dedicated to micro-decarburization hardening grinding based on gas-protecting coupling method is designed and established. WE6800-ZC surface grinder is chosen as the foundation. The nitrogen is chosen as the protective gas, owing to its exceptional chemical stability, inertness towards carbon elements, ready availability, and favorable economics. The nitrogen cylinder, strategically positioned adjacent to the grinder, serves as the primary source of the protective gas, which is then channeled through a dedicated gas conduit.

Recognizing that coolant is not a necessity in grinding hardening processes and noting the original coolant outlet's strategic location at the interface between the grinding wheel and workpiece, this outlet is repurposed ingeniously as the gas ejection port. This approach ensures that the protective nitrogen gas is precisely directed towards the critical grinding area, minimizing the risk of decarburization. To facilitate this seamless transition, the original coolant conduit is meticulously disconnected from the grinder's coolant container and seamlessly connected to the nitrogen cylinder's gas conduit. This intricate reconfiguration enables dynamic ejection of the protective gas, intricately synchronized with the grinding wheel's movement. The whole resulting experimental platform is shown in Fig. 1.

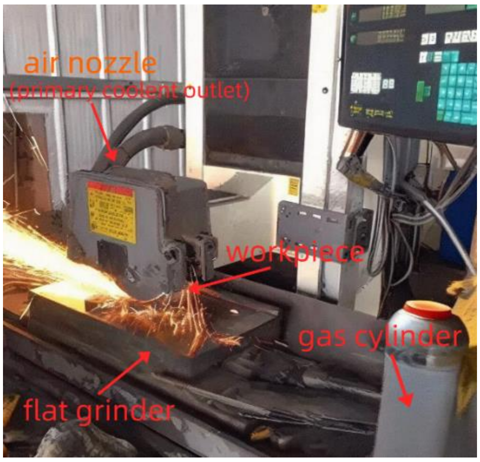

Figure1 Experimental platform

Upon the completion of platform of the slight decarburization grinding hardening based on the gas-protecting coupling method, a series of meticulous grinding experiments are embarked upon under diverse operational conditions. Specifically, 45 steel workpiece is meticulously selected. The size of specimen is 60mm×15mm×15mm. They are subjected to grinding processes under two primary scenarios: one with protective gas injection and another without, offering a direct comparison of their respective impacts. Furthermore, to delve deeper into the process dynamics, the grinding depth is systematically varied, enabling the evaluation of its influence on the decarburization and hardening outcomes. This comprehensive approach aimed to unravel the intricate interplay between process parameters, gas composition, and material properties, ultimately leading to optimized micro-decarburization hardening processes. The whole experiment condition is shown in Table 1.

Table 1 Experiment condition

No.	a_p[μm]	v_s[m/s]	v_w[m/s]	grinding wheel	grinding width	coolant	gas protection
1	150	0.02	40	F46	15mm	no	yes
2	150	0.02	40	F46	15mm	no	no

2.2 Experiment result and analysis

Utilizing electron probe microanalysis, the carbon content on the workpiece surface of various groups after grinding is meticulously quantified, yielding results as illustrated in Fig. 2. Notably, the workpiece subjected to gas-protected micro-decarburization hardening grinding exhibited a markedly elevated carbon content on their surfaces compared to those hardened solely through grinding. This observation underscores the efficacy of the gas-composite protection strategy in effectively mitigating decarburization during the grinding process. By inhibiting the undesirable loss of carbon from the surface, this innovative approach not only ensures the desired hardening effect but also achieves a surface hardening layer characterized by minimal decarburization. Thus, the experiment validates the successful implementation of micro-decarburization hardening grinding with gas-composite protection, marking an advancement in surface treatment techniques aimed at optimizing material properties and enhancing durability.

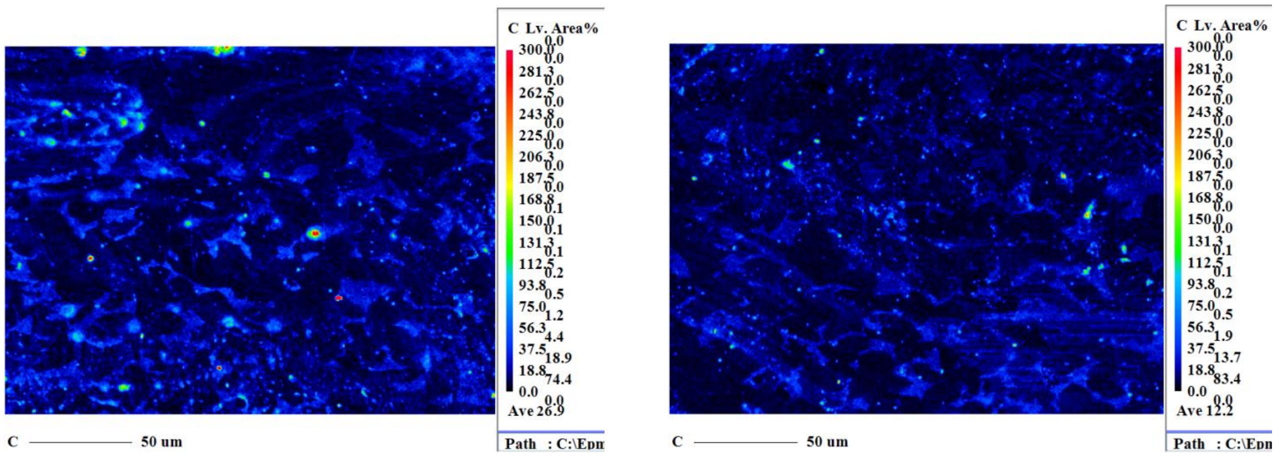

(a) gas-protected hardening grinding (b) grinding hardening

Figure 2 Carbon content on the surface of workpiece after grinding

3 Study on coupling airflow-field

3.1 Establishment of airflow-field model

During the intricate grinding process, the vigorous rotation of the grinding wheel generates a viscous action on its surface, propelling the adjacent air into a vortex. This phenomenon results in the formation of a dynamic, high-velocity, high-pressure, and robust airflow layer enveloping the grinding wheel's surface[17-19]. This airflow layer poses a significant challenge as it disrupts the smooth flow of the shielding gas jet, impeding its effective penetration into the crucial grinding area[20]. To address this issue and ensure optimal performance, a comprehensive study is conducted on the intricate coupling field between the shielding gas and the rotating air generated by the grinding wheel. By establishing detailed gas flow field models for both up-grinding and down-grinding contact areas, the effective flow rate of the sprayed shielding gas is calculated precisely. This analysis facilitated the design of strategic gas jets, tailored to overcome the disruptive effects of the surrounding airflow and ensure efficient delivery of the shielding gas directly into the grinding zone. Furthermore, the research delved into the intricate mechanisms underlying the comprehensive protection offered by varying gas jet flow fields. By elucidating the complex interactions between the shielding gas, rotating air, and grinding process dynamics, valuable insights are gained into optimizing the shielding gas system for maximum effectiveness and efficiency. This, in turn, contributes to the development of advanced grinding technologies capable of achieving superior surface quality and minimal decarburization, thereby enhancing the overall performance and longevity of the ground components.

The coupling field between grinding wheel and jet gas is established based on Fluent of ANSYS. First, a three-dimensional model of grinding wheel, jet gas and workpiece are established, as shown in Fig. 3. The coupling part of grinding wheel participating in gas field is equivalent to a cambered surface.The workpiece is set as the bottom surface, and the gas injection port is preliminarily set as a circular nozzle, which is located between the grinding wheel and the workpiece. The injection port is set as the entrance of fluent. The grinding wheel arc surface is set as the rotating wall surface. The workpiece is set as the static wall surface. The other surfaces are set as the outlets.

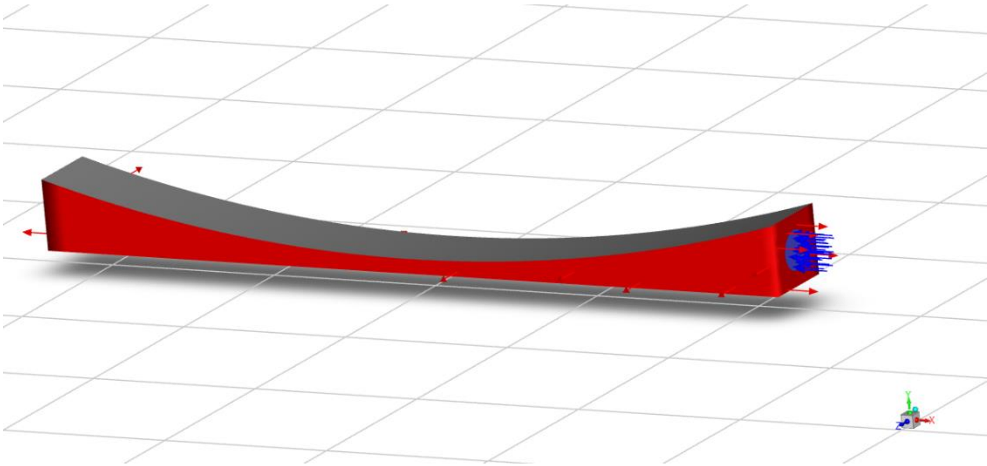

Figure 3 Three-dimensional model of coupling gas field

Secondly, the three-dimensional model is meshed. In order to improve the calculation accuracy and reduce the calculation time, the meshes at the entrance, adjacent workpiece and grinding wheel workpiece are properly encrypted.

After modeling and meshing, the simulation parameters and conditions are set. Because the collision between the rotating air flow and the jet gas is in a relatively stable state after stabilization, and does not change with time, the simulation time type is set as steady state. Considering the influence of gravity, according to the coordinate axis setting, the initial value in Y direction is set to -9.81 m/s. Because the airflow collision involves nitrogen and conventional air, the VOF function of multiphase flow is turned on, and the nitrogen in fluent material library is added to the fluid part of material setting accordingly. The viscous model is set to k-epsilon type, which can be used to calculate most fluid problems, and the system default values are selected for the parameters. The type of grinding wheel wall is set as moving wall. The type is selected as rotating wall. The rotation axis coordinate is the center coordinate of grinding wheel. The rotation speed of the wall is initially set as 20rad/s. The rough cross-over height and roughness constant of the wall are set with reference to the surface value of grinding wheel. The workpiece is set as a static wall, and the parameters adopt default values. The gas injection inlet type is set as pressure inlet according to the actual working condition, and the initial setting is 30000Pa. The turbulence diameter is consistent with the injection inlet diameter, and the model is set as 2mm. The remaining surfaces are set as outlets, and the type is set as pressure outlets. The value is set as a standard atmospheric pressure. After setting the parameters, the model is initialized, whose type is standard initialization. After initialization, the animation type of the result is adjusted to pressure nephogram. It can be seen that the injection port is ready for pressure at this time. The number of iteration steps and iteration interval are set. 200 iteration steps are selected, and the calculation is start.

3.2 Analysis of coupling airflow field

Upon reaching a steady state following the simulation calculations, the intricate coupling dynamics between the rotating airflow of the grinding wheel and the injected jet airflow are vividly illustrated in Fig. 4. This state signifies the full activation and subsequent equilibrium of both airflow systems. Notably, the region adjacent to the nozzle, where the grinding wheel resides, experiences the highest pressure, indicative of the concentrated interaction between the two airflow phenomena. Conversely, the immediate vicinity between the grinding wheel and the workpiece registers the lowest pressure, possibly due to the turbulent mixing and redirection of airflows. The pressure at the remaining two extremities of the grinding zone falls into an intermediate range, reflecting a smoother transition.

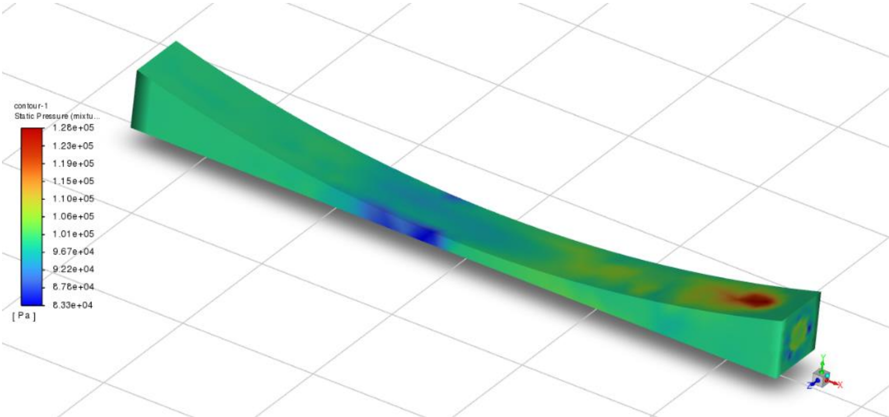

Figure 4 Coupling results of grinding wheel rotating airflow and jet airflow

The characteristics of coupled gas field are revealed further. A new plane is constructed along the XY plane direction in the middle of the simulation model, and the pressure of this plane is plot by using fluent drawing function. The results are shown in Fig.5. The pressure increases rapidly at the rightmost end, then decreases gradually through the air flow attenuation to the left, and then further decreases near the center line, forming a relative negative pressure area, which is caused by the rotating air flow of grinding wheel. Then it gradually rises to the left and then slowly, approaching atmospheric pressure. The coupling gas field synthesis forms this feature.

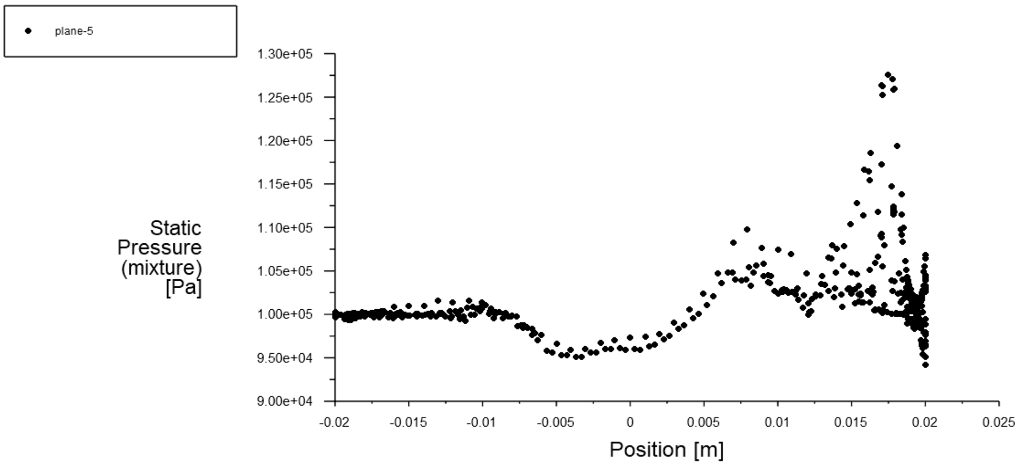

Figure 5 Result of pressure of XY plane(rotation speed=20rad/s, injection pressure=3000000Pa)

4 Prediction model of decarburization control

The development of a predictive model for the slight decarburization grinding hardening based on the gas-protecting coupling method necessitates a meticulous approach leveraging the power of neural networks[21]. This model aims to accurately forecast the carbon content within the surface layer of components subjected to varying grinding parameters and gas characteristics, thereby providing a quantitative assessment of the decarburization control's efficacy. The modeling process commences with a meticulous data collection and preprocessing phase, outlined as follows:

4.1 Data Collection and Preprocessing

The cornerstone of this endeavor lies in the systematic gathering of experimental data pertaining to the slight decarburization grinding hardening based on the gas-protecting coupling method. This involves meticulously recording the carbon content within the surface layer of workpiece under diverse conditions, particularly varying gas pressures and grinding depths. Given the inherent costliness of conducting such experiments and measuring carbon content accurately, a judicious selection of 18 comprehensive datasets, each representing unique conditions, is made. The data is presented in Table 2.

Table 2 Experimental data of C content of Slight Decarburization Grinding Hardening

P[MPa] \ a_p [μm]	100	125	150
1	0.027	0.026	0.022
2	0.031	0.028	0.027
3	0.032	0.033	0.031
4	0.036	0.037	0.035
5	0.037	0.037	0.036
6	0.038	0.039	0.038

To ensure the integrity of the modeling process, the collected data undergoes rigorous cleaning, where outliers or erroneous records are identified and eliminated. This step is crucial to mitigate the potential for biased predictions. Subsequently, normalization is applied to the refined dataset, scaling the input values to fall within the neural network's preferred range of [-1, 1]. This normalization not only facilitates faster training convergence but also enhances the model's generalization capabilities. Finally, the preprocessed data is partitioned into two distinct sets: a training set and a validation set. The training set serves as the primary source of information for the neural network to learn and develop its predictive capabilities, while the validation set is reserved for assessing the model's performance on unseen data, ensuring its robustness and reliability. This strategic division ensures that the model is not merely memorizing the training data but is genuinely capable of making accurate predictions under varying conditions.

4.2 Neural Network Model Design

A deep fully connected neural network (FCN) is designed. Considering the complex and nonlinear effects of gas pressure and grinding depth on carbon content, a neural network with multiple hidden layers is chosen[22]. The Sequential model, which is a linearly stacked model, is used. The input layer receives two variables, namely gas pressure and grinding depth. The output layer has one neuron, corresponding to the carbon content in the surface layer of the workpiece. The model contains two hidden layers, each with three neurons, and uses the Sigmoid activation function. The whole structure of FCN is shown in Fig. 6.

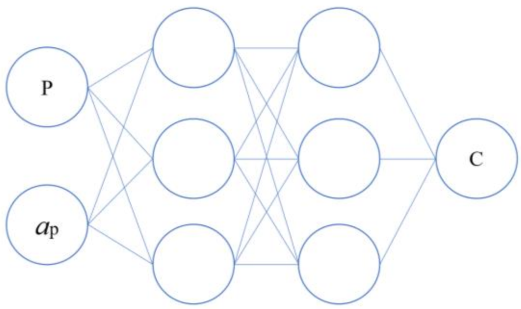

Figure 6 structure of FCN

4.3 Model Training

Mean Squared Error (MSE) is chosen as the loss function to assess the difference between predicted and actual values. Adam is selected as the optimization algorithm to adjust network weights to minimize the loss function.

The neural network is trained using the training set data. Prediction values are calculated through forward propagation, and network weights are updated through backpropagation. Performance on the validation set is monitored to prevent overfitting.

4.4 Model Evaluation and Analysis

The comparison of prediction results against experimental data, as depicted in Fig. 7, reveals a close correspondence between the two, signifying the model's predictive prowess. However, minor deviations are discernible, which can be attributed to several factors. Firstly, the randomness in the initial weights and biases of the neural network introduces variability. As different initialization methods may steer the model towards distinct local optimal solutions, this contributes to prediction uncertainties. Furthermore, the precision of electronic probe measurements, while high, is not absolute, leading to inherent measurement errors that propagate into the prediction model.

Despite these limitations, the trained model offers valuable insights into the decarburization process. It enables the prediction of carbon content in workpiece surface layers under various gas pressures and grinding depths, thereby empowering process engineers to make informed decisions. By adjusting process parameters in real-time based on the model's predictions, engineers can fine-tune the decarburization control to achieve optimal outcomes. This predictive capability fosters efficiency, reduces waste, and ensures consistent product quality, ultimately enhancing the competitiveness of the manufacturing process.

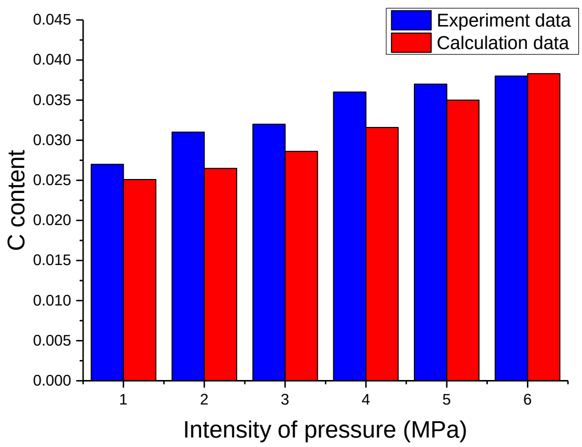

Figure 7 Differences between the prediction results and experimental values

Conclusion

The research developed a novel grinding hardening method that utilizes a gas-protecting coupling technique to control decarburization, resulting in enhanced mechanical properties of the machined workpiece. The gas composite shielding micro-decarburization hardening grinding method prevents surface decarburization. The experimental results validate the effectiveness of the protective gas in maintaining the carbon content on the workpiece surface, leading to a better hardening effect.

The airflow-field study provided insights into the dynamics of the shielding gas and its interaction with the grinding wheel's rotating airflow, offering a theoretical basis for optimizing the gas injection parameters. The developed neural network model accurately predicts the carbon content under different conditions, serving as a valuable tool for adjusting process parameters and ensuring the precision of decarburization control.

In conclusion, the integration of gas-protecting coupling in the grinding hardening process presents a significant advancement in the field of abrasive machining, offering a green, efficient, and precise method for improving the surface quality of carbon steel workpiece. This research contributes to the optimization of grinding processes and the enhancement of workpiece performance, with potential applications in various industrial sectors.

Ackolodgement

This paper is supported by the National Natural Science Foundation of China(Grant No. 52205452).

Reference

1. Brinksmeier, E., Brockhoff, T., Surface heat treatment by using advanced grinding processes. *Metallurgia Italiana*, 1999, 91(4): 19~23.
2. Thang, V.T., Tuan, N.A., Tiep, N.V., Evaluation of grinding wheel wear in wet profile grinding for the groove of the ball bearing's inner ring by pneumatic probes. *J*

Mech Sci Technol, 2018, 32(3): 1297-1305.

3. Zhu, X.L., Li, Y., Dong, Z.G., Kang, R.K., Gao, S., Study into grinding force in back grinding of wafer with outer rim. Adv Manuf, 2020, 8(3):361-368.
4. Thanedar, A., Dongre, G.G., Singh, R., Joshi, S.S. Surface integrity investigation including grinding burns using barkhausen noise (BNA). *J Manuf Processes*, 2017, 30: 22 6-240.
5. Zhang, Y.B., Li, C.H., Jia, D.Z., Li, B.K., Wang, Y.G., Yang, M., Hou, Y.L., Zhang, X.W. Experimental study on the effect of nanoparticle concentration on the lubricating property of nanofluids for MQL grinding of Ni-based alloy. *J Mater Process Tech*, 2016, 232: 100-115.
6. Fang, M.H., Yu, T., Xi, F.F. Effect of back pressure on the grinding performance of abrasive suspension flow machining. *Adv Manuf*, 2022, 10(1):143-157.
7. Nguyen, T., Zhang, L.C., Sun, D.L., Wu, Q., Characterizing the mechanical properties of the hardened layer induced by grinding-hardening. *Mach Sci Technol*, 2014, 18(2): 277-298.
8. Huang, X.M., Ren, Y.H., Zheng, B., Deng, Z.H., Zhou, Z.X., Experiment research on grind-hardening of AISI5140 steel based on thermal compensation. *J Mech SciI Technol*, 2016, 30(8): 3819-3827.
9. Zhang, Y., Ge, P.Q., Be, W.B., Plane grind-hardening distortion analysis and the effect to grind-hardening layer. *Int J Adv Manuf Technol*, 2015, 78(1-4): 431-438.
10. Xiu, S.C. and Shi, X.L. Transformation mechanism of microstructure and residual stress within hardening layer in PSHG. *J Adv Mech Des Syst* 2015, 9(3): 15-00288.
11. Liu, M., Nguyen, T., Zhang, L.C.,Wu, Q., Sun, D., Effect of grinding-induced cyclic heating on the hardened layer generation in the plunge grinding of a cylindrical component. *Int J Mach Tools Manuf*, 2015, 8 9: 55-63.
12. Alonso, U., Ortega, N., Sanchez, J.A., Pombo, I., Izquierdo, B., Plaza, S. Hardness control of grind-hardening and finishing grinding by means of area-based specific energy. *Int J Mach Tools Manuf*, 2015, 88: 24-33.
13. Wang, G.B., Cheng, G.G., Zhang, Y.L., Ruan, Q., Pan, J.X., Chen, X.R., A Dynamic Decarburization Model in Vacuum Oxygen Decarburization Process for Ultrapure Ferritic Stainless Steel. *Steel Res Int*, 2023, 94(11).
14. Zhan, D.P., Zhang, Y.P., Jiang, Z.H., Zhang, H.S., Model for Ruhrstahl-Heraeus (RH) decarburization process. *J Iron Steel Res Int*, 2018, 25(4): 409-416.
15. Luo, H.W., Xiang, R., Chen, L.F., Pan, L.M., Modeling decarburization kinetics of grain-oriented silicon steel. *Chin Sci Bull*, 2014, 59 (15): 1778-1783.
16. Van, Hall, S.N., Findley, K.O., Freis, A.K., Improved self-pierce rivet performance through intentional decarburization. *J Mater Process Technol*, 2018, 251: 350-359.
17. Zou, X.N., Zhang, G,S., Li, Q.L., Xiu, S.C., Kong, X.N., Yao, Y.L., Flow field analysis of grinding fluid in double-face grinding. *Int J Adv Manuf Technol 2024*, 131(5-6): 2071-2085.
18. Mandal, B., Singh, R., Das, S., Banerjee, S., (2011) Improving grinding performance by controlling air flow around a grinding wheel. *Int J Mach Tools Manuf*, 2011, 51(9): 670-67 6.
19. Ji, T., Huang, S.L., Ren, B.M., Ye, J.Z,, Wang, G.W. Analysis of grinding fluid flow in high-temperature alloy surface profile grinding. *Int J Adv Manuf Technol*, 2023, 124 (3-4): 759-771.
20. Li, C.H., Zhang, Q., Wang, S., Jia, D.Z., Zhang, D.K., Zhang, Y.B., Zhang, X.W., Useful fluid flow and flow rate in grinding: an experimental verification. *Int J Adv Manuf Technol*, 2015, 81(5-8): 785-794.
21. Young, T.R., Lichtenberg, A.A., Benjamin, S., Neural Networks and Neural Networks: Start Making Sense. *J Neuropsychiatry Clin Neurosci*, 2020, 32(3): E26-E26.
22. Huang, H., Li, J.Q., Wang, M., Wang, H. FCN-Based Carrier Signal Detection in Broadband Power Spectrum. *IEEE Access*, 20 20, 8: 113042-113051.